A global sensitivity analysis of model uncertainty in aeroelastic wind turbine models

Prashant Kumar, Benjamin Sanderse

[a]*Centrum Wiskunde & Informatica (CWI), Amsterdam, The Netherlands*

Abstract

A global sensitivity analysis of model parameters associated with the Blade Element Momentum (BEM) models is performed. The Sobol indices based on a sparse polynomial expansion are used as a measure of global sensitivities. The sensitivity analysis workflow is developed using the uncertainty quantification toolbox `UQLab` that is integrated with the ECN's `Aero-Module` aeroelastic code. Sensitivity studies are performed on the NM80 wind turbine model from the DANAERO project.

Keywords: BEM, global sensitivity analysis, model uncertainty, Sobol indices

1. Introduction

Aeroelastic models such as the Blade Element Momentum (BEM) models [4] play a critical role in the design, development, and optimization of modern wind turbines. A large number of BEM models have been developed to predict turbine responses such as the structural loads and power output [26].

As a consequence of the strong model assumptions at the basis of BEM theory, the results from BEM codes can be subject to significant inaccuracies or uncertainties. For example, the effect of sheared inflow [12] is not naturally accounted for in the theory and needs to be incorporated via correction terms. Other major model uncertainties in BEM models are for example the time constant in dynamic stall models, the wake correction factor, the tip loss model parameter, and the lift- and drag-polars used to compute local aerodynamic forces. Especially for increasing turbine sizes, these model parameters are foreseen to be not sufficiently accurate [21]. In other words, the uncertainty associated with the output of currently employed BEM models is rather large.

Recently, several papers have addressed the uncertainty in BEM model output by performing forward uncertainty propagation or sensitivity studies, e.g. [7, 14, 16, 19, 24]. In these studies, the focus in mainly on uncertainties in the external conditions (wind parameters) and/or uncertainty in the turbine specification (geometric parameters). Apart from understanding how uncertainty in the output is related to the different uncertain inputs, such sensitivity studies are very useful to reduce the number of parameters as needed for example in design optimization [7]. However, the uncertainty in BEM model output as caused by uncertainty in the model formulation itself, e.g. through the values chosen for model parameters, has been given little attention (exceptions being the effect of aerodynamic properties studied in [2, 14])this is also what we do.

The goal of this work is to perform a systematic assessment of the uncertainty in model parameters in BEM models. We approach this by performing a global sensitivity analysis based on the Sobol expansion approach, which decomposes the total variance of the quantity of interest (model output) into contributions from individual parameters and their combinations, similar to [7, 16, 18]. We will employ the uncertainty

Email address: `pkumar@cwi.nl` (Prashant Kumar)

quantification toolbox UQLab [13], which computes the Sobol indices based on a sparse polynomial chaos expansion.

The main novelty of the work lies in the study of the effect of model uncertainties rather than external conditions or geometric uncertainties. As such, the current sensitivity analysis is part of the so-called WindTrue project, in which the long-term goal is the development of calibrated BEM models, that possess a quantified level of uncertainty. Anticipating on this goal, we are using the NM80 wind turbine model from the Tjaereborg wind farm, for which extensive measurement data is available through the DanAero project [23] and IEA Task 29. The measurement data will enable the calibration step, and our sensitivity analysis will make clear which of the model parameters should be used in this calibration step.

This paper is structured as follows. First, in section 2 we give a short description of the BEM model and associated geometric and model uncertainties. In section 3 the parameterization of the uncertainties is described, and in section 4 the global sensitivity analysis methodology. Section 5 discusses the results of the sensitivity analysis for the NM80 turbine test case, and conclusions follow in section 6.

2. Aeroelastic model uncertainties

State-of-the-art wind-turbine models simulate the aeroelastic behavior of wind turbines by combining the concept of momentum conservation of the flow (BEM theory) with the equations of motion for the structure, possibly extended with the hydrodynamics of the sea and control algorithms [26]. In this work, we only concentrate on the first aspect, namely the prediction of flow and blade forces as given by the BEM method. The particular BEM code that we use is ECN's Aero-Module [1].

For the case of a rigid turbine, with a uniform inflow field, the main model uncertainties that arise in the BEM formulation are the following [10]:

- The use of (2D) *airfoil polars*; uncertainty arises not only because the actual flow along the blade is 3D, but also because the 2D polars itself can be inaccurate, either when obtained from measurements or 2D codes like XFOIL;
- The assumption of locally 2D flow along the blade is also invalid at the tip; this is typically corrected via *a tip loss model*;
- Three-dimensional flow effects also cause stall delay at the root; this is typically modeled via *a dynamic stall model* and associated time constant;
- Yawed inflow is not naturally included in BEM and typically incorporated via *a wake correction*.

Next to these model uncertainties we will consider the chord and twist distribution along the blade to be uncertain (geometric uncertainties).

3. Parametrization of uncertain inputs

The chord, twist, lift coefficient, and drag coefficient are functions of the radial distance along the blade, leading to a very high-dimensional number of uncertain parameters. In order to reduce this number, we parametrize the variation along the blade by using Non-Uniform Rational Basis Splines (NURBS) [20]. In this way only a limited number of control points is needed to approximate a large variety of curves, so that the resulting number of uncertain parameters is relatively small. NURBS have already been exploited in several aerodynamics applications, for instance, design optimization of wind-turbine blades, e.g. [3, 17], and to parametrize chord and twist curves [7]. In the following, we briefly outline the procedure used to parametrize a curve using NURBS.

3.1. NURBS representation

A NURBS curve $S(x)$ is expressed using a weighted sum of n basis functions (or B-splines):

$$S(x) = \sum_{i=1}^{n} c_i B_{i,p}(x), \tag{3.1}$$

where c_i is the weight of the i-th control point and $B_{i,p}(x)$ is the value of the B-spline corresponding to the i-th control point at x, with the subscript p denoting its polynomial degree. In our case, $S(x)$ represent for example the chord as a function of the radial location along the blade. A sequence of non-decreasing parameters $X = \{x_1, x_2, ..., x_m\}$, called the *knot vector*, determines the domain in which any control point is active. A control point c_i is said to be active at a location when the corresponding B-spline $B_{i,p}(x)$ is non-zero at x. B-splines are recursive in polynomial degree, thus we can derive quadratic B-splines using linear B-splines, cubic from quadratic B-splines and so on. Starting with a B-spline of degree 0 defined as

$$B_{i,0}(x) := \begin{cases} 1 & x_i \le x < x_{i+1}, \quad i = 1, 2, ..., m, \\ 0 & \text{elsewhere}, \end{cases} \tag{3.2}$$

we can derive higher-order B-splines using the recurrence relation [5]:

$$B_{i,p}(x) := \frac{x - x_i}{x_{i+p} - x_i} B_{i,p-1}(x) + \frac{x_{i+p+1} - x}{x_{i+p+1} - x_{i+1}} B_{i+1,p-1}(x), \quad p \ge 1. \tag{3.3}$$

Note that with increasing p the interval in which a B-spline is non-zero also become larger. For a curve of polynomial degree p, there are $p + 1$ active control points at any location x. For example, for a linear curve ($p = 1$) only two adjacent control points are active at any location. Therefore, only a few nearby control points are active when computing the NURBS curve (3.1). These B-splines can be constructed efficiently using the de Boor's algorithm [5]. To compute high-order B-splines in (3.3), we need to pad the knot vector X by repeating the first and last elements p times each. In Fig. 1, we show linear, quadratic and cubic splines for $x \in [0, 1]$ with original knot vector $X = \{0, 1/3, 2/3, 1\}$, padded accordingly with the curve order, for e.g., for linear B-splines, we use the knot vector $X = \{0, 0, 1/3, 2/3, 1, 1\}$.

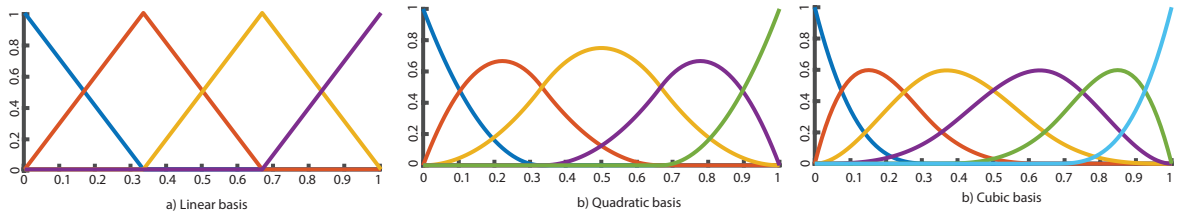

Figure 1: Examples of B-splines with original knot vector $X = \{0, 1/3, 2/3, 1\}$.

In order to parameterize a given curve, e.g. the blade reference chord, we choose a degree p and a number of knots $X = \{x_j\}_{j=1}^{n}$. The knots can be uniformly spaced or chosen heuristically (for advanced approaches for knot selection see[**? ?**]). Next we sample $S_{ref}(x)$ at X and also compute $B_{i,p}(x_j)$, for $i, j = 1, 2, ..., n$. We then formulate a linear system and solve for the set of control points $\mathbf{c} = \{c_i\}_{i=1}^{n}$ as:

$$\mathbf{Bc} = \mathbf{S}_{ref}, \tag{3.4}$$

where $\mathbf{S}_{ref} \in \mathbb{R}^n$ is a vector containing sampled values of $S_{ref}(x)$ and $\mathbf{B} \in \mathbb{R}^{n \times n}$ is a matrix with the j-th row consisting of values of n B-splines sampled at location x_j. Once the control points are obtained, the approximate reference curve $S_n(x)$ follows from (3.1). Fig. 2 shows a parameterization of the chord curve using $n = 9$ control points and second-order ($p = 2$) B-splines.

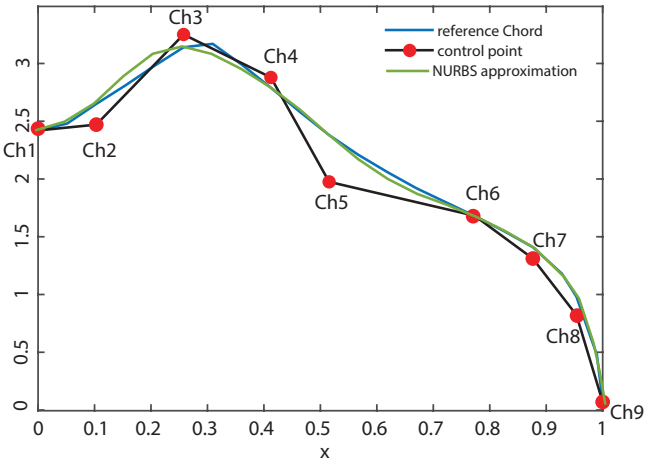

Figure 2: Parametrization of chord using 9 control points and second-order B-splines.

3.2. Perturbing the NURBS curves

Given the reference values of $\mathbf{c}$, it becomes straightforward to generate perturbed curves: we sample a uniform random variable to perturb the baseline control points and use these to compute a perturbed curve $\tilde{S}(x)$:

$$\tilde{S}(x) = \sum_{i=1}^{n} \tilde{c}_i B_{i,p}(x), \tag{3.5}$$

where

$$\tilde{c}_i = c_i(1 + \Delta_i), \tag{3.6}$$

and the perturbation is randomly sampled as $\Delta_i \sim \mathcal{U}[-0.05, 0.05]$.

3.3. Model uncertainties

The above framework is directly applicable to express the geometric uncertainty in twist- and chord distribution, with c denoting either the value of the twist control points or of the chord control points. For model uncertainties, i.e. lift- and drag polars, Insert mathematical expression

4. Global sensitivity analysis

The objective of sensitivity analysis is to quantify the relative significance of individual inputs (or their combination) and how variations in input values affect the output of interest. Sensitivity analysis techniques can be classified as local and global [22]. In a local sensitivity analysis, individual parameters are perturbed around their nominal values allowing for the description of output variability only in a small neighbourhood around the nominal input values. Although local approaches are widely employed due to their ease of implementation and low computational cost, they are unable to quantify the global behaviour of nonlinearly parametrized models such as aeroelastic models. Global sensitivity approaches, on the other hand, consider the entire range of input values to compute output sensitivities. Therefore, a global sensitivity analysis is more suitable for the aeroelastic models considered in this work.

4.1. Sobol analysis

We employ the variance-based Sobol decomposition to perform global sensitivity analysis. This approach allows for quantification of the relative importance of the input parameters on a scale of $[0, 1]$ known as *Sobol indices*. In a Sobol analysis, we express the total variance of the output in term of contributions from individual parameters and their combinations. Consider a generic BEM model $f(\mathbf{z})$, depending on uncertain parameters $\mathbf{z}$ and returning a quantity of interest Y (e.g. power, loads, moments):

$$Y = f(\mathbf{z}), \tag{4.1}$$

where $\mathbf{z} = [z_1, z_2, ..., z_M] \in \mathcal{D}_\mathbf{z} \in \mathbb{R}^M$ is a vector of random variables (parameters). For ease of notation, we assume these input parameters to be uniformly distributed i.e. $z_i \sim \mathcal{U}(0, 1)$ and the support of the input set is $\mathcal{D}_\mathbf{z} = [0, 1]^M$ where M is the total number of input parameters. The Sobol decomposition is based on the following hierarchical representation [22]:

$$f(z_1, z_2, ..., z_M) = f_0 + \sum_{i=1}^{M} f_i(z_i) + \sum_{1\le i<j\le M} f_{ij}(z_i, z_j) + ... + f_{1,2,...,M}(z_1, z_2, ..., z_M). \tag{4.2}$$

Here the zeroth-order function f_0 is the mean response of f, the first-order univariate functions $f_i(z_i)$ quantify independent contributions due to each random input, and second-order functions $f_{i,j}(z_i, z_j)$ represent the effect of interaction between z_i and z_j on the response f. Formally, the zeroth-, first- and second-order terms are defined as:

$$f_0 = \int_{\mathcal{D}_\mathbf{z}} f(\mathbf{z}) d\mathbf{z}, \tag{4.3}$$

$$f_i(z_i) = \int_{\mathcal{D}_\mathbf{z}^{M-1}} f(\mathbf{z}) d\mathbf{z}_{\sim\{i\}} - f_0, \tag{4.4}$$

$$f_{ij}(z_i, z_j) = \int_{\mathcal{D}_\mathbf{z}^{M-2}} f(\mathbf{z}) d\mathbf{z}_{\sim\{i,j\}} - f_i(z_i) - f_j(z_j) - f_0, \tag{4.5}$$

where $\mathcal{D}_\mathbf{z}^{M-1} = [0, 1]^{M-1}$ and the notation $\mathbf{z}_{\sim\{i,j\}}$ denotes the vector having all the components of $\mathbf{z}$ except in the set $\{i, j\}$. Higher-order terms are interpreted in a similar manner. Note that (4.2) is only valid for independent input parameters. We only consider a second-order expansion of (4.2), as for many applications this is sufficient because higher-order terms have negligible effect on the output response.

As an example, Y can represent the power output of a wind turbine, with random inputs windspeed (z_1), wind standard deviation (z_2) and rotational speed (z_3). f_0 then represents the mean power output considering all the three random inputs, $f_1(z_1)$ represent the independent contribution of windspeed on the power and $f_{1,2}(z_1, z_2)$ quantifies the interactions of wind speed and wind standard deviation on power.

The definition of the variance is:

$$D = \mathrm{Var}[f(\mathbf{z})] = \int_{\mathcal{D}_\mathbf{z}} f^2(\mathbf{z}) d\mathbf{z} - f_0^2. \tag{4.6}$$

As the expansion in (4.2) is not unique, some orthogonality conditions must be imposed [**? ?**] which allows to express the total variance as

$$D = \sum_{i=1}^{M} D_i + \sum_{1\le i<j\le M} D_{ij}, \tag{4.7}$$

where the first- and second-order partial variances are defined via the Sobol decomposition as

$$D_i = \int_0^1 f_i^2(z_i) dz_i, \qquad D_{ij} = \int_0^1 \int_0^1 f_{ij}^2(z_i, z_j) dz_i dz_j. \tag{4.8}$$

The first- and second-order Sobol indices are then computed as

$$S_i = \frac{D_i}{D}, \quad S_{ij} = \frac{D_{ij}}{D}, \quad i, j = 1, 2, ..., M. \tag{4.9}$$

The total effect of z_i on the output Y can be quantified using the total sensitivity index

$$S_{T_i} = S_i + \sum_{j=1}^{M} S_{ij}. \tag{4.10}$$

The total sensitivity indices can be interpreted as an importance measure for the parameter z_i, therefore a large S_{T_i} implies that z_i has a strong influence on Y. The computation of S_{T_i} requires the approximation of partial variances defined in (4.9). Using the Monte Carlo method for computing these variances can be prohibitive for computationally expensive models Y. On the other hand, Polynomial Chaos Expansions (PCE) based approaches provide a more efficient alternative for sensitivity analysis, and will be used here. As shown in [**?**], one can compute the Sobol indices analytically by post-processing the PCE coefficients.

4.2. PCE-based Sobol indices computation

The PCE approximation $f^K(\mathbf{z})$ of the computational model Y can be defined as a weighted sum of multivariate polynomials in $\mathbf{z}$ [22]

$$Y = f(\mathbf{z}) \approx f^K(\mathbf{z}) = \sum_{|\mathbf{k}|=0}^{K} w_{\mathbf{k}} \Psi_{\mathbf{k}}(\mathbf{z}), \tag{4.11}$$

where $\mathbf{k} \in \mathbb{N}_0^M$ is a M-dimensional multi-index with magnitude $|\mathbf{k}| = k_1 + k_2 + ... + k_M$ and $\Psi_{\mathbf{k}}(\mathbf{z})$ a multivariate polynomial basis, which is computed using a tensor product of univariate polynomials $\psi_{k_i}^{(i)}(z_i)$

$$\Psi_{\mathbf{k}}(\mathbf{z}) := \prod_{i=1}^{M} \psi_{k_i}^{(i)}(z_i), \tag{4.12}$$

where k_i is the order of the univariate polynomial. The choice of the univariate orthogonal polynomial ψ_{k_i} depends on the type of random variable, z_i. For example, for uniform random variables the Legendre family of polynomials is used [**?**]. The total number of terms K in (4.13) can be based for example on a standard truncation scheme in which all polynomials in M random variable with order less than or equal to p are used. More advanced truncation schemes such as the maximum interaction or a hyperbolic scheme can also be employed depending on the application, see [**?**]. which one is used?

The PCE coefficients $w_{\mathbf{k}}$ corresponding to $\Psi_{\mathbf{k}}(\mathbf{z})$ can be computed using a pseudo-spectral approach by using quadrature methods. For a small number of dimensions this is an efficient approach. However, in the current work we will encounter more than 10 dimensions and quadrature methods are typically too expensive as they suffer strongly from the curse of dimensionality. We therefore focus on methods in which the sampling points can be chosen more freely: Ordinary Least Squares (OLS) and Least-Angle Regression (LARS).

4.2.1. Ordinary Least Squares

Instead of using a projection-based method one can also use least squares based approaches to compute coefficients [**?**]. The PCE expansion (4.13) can be expressed as a vector-matrix product

$$Y = f^K(\mathbf{z}) + \varepsilon_K = \sum_{|\mathbf{k}|=0}^{K} w_{\mathbf{k}} \Psi_{\mathbf{k}}(\mathbf{z}) + \varepsilon_K = \mathbf{w}^T \mathbf{\Psi}(\mathbf{z}) + \varepsilon_K, \tag{4.13}$$

where $\mathbf{w} = \{w_0, w_1, ..., w_K\}^T$ is the coefficient vector, $\mathbf{\Psi}(\mathbf{z}) = \{\Psi_0(\mathbf{z}), \Psi_1(\mathbf{z}), ..., \Psi_K(\mathbf{z})\}^T$ is the matrix containing multivariate polynomials in $\mathbf{z}$, and ε_K is the approximation error. The least-squares minimization problem can then be formulated as:

$$\overline{\mathbf{w}} =_{\mathbf{w}} \mathbb{E}\left[\left(\mathbf{w}^T\mathbf{\Psi}(\mathbf{z}) - f(\mathbf{z})\right)^2\right] \tag{4.14}$$

The coefficient vector $\overline{\mathbf{w}}$ can be computed using the Ordinary Least Squares (OLS) method. Given N model evaluations $\mathbf{Y} = \{f(\mathbf{z}_1), f(\mathbf{z}_2), ..., f(\mathbf{z}_N)\}$, we can obtain the coefficients as:

$$\overline{\mathbf{w}} = (\mathbf{X}^T\mathbf{X})^{-1}\mathbf{X}^T\mathbf{Y}, \tag{4.15}$$

where $\mathbf{X} \in \mathbb{R}^{N\times K}$ is the design matrix where $\mathbf{X}_{i,j} = \Psi_j(\mathbf{z}_i)$, $i = 1, 2, ..., N$ and $j = 0, 1, 2, ..., K$. Although the OLS method allows to compute the coefficients using a limited number of model evaluations, one of the main drawbacks of this approach is that it may result in a PCE model that consists of high-order interaction terms that may lead to overfitting. For many engineering problems, low-order interactions between the input variables are most important. Therefore, the least squares form in (4.17) can be regularized such that the minimization results is a low-order sparse PCE model, as discussed next.

4.2.2. Least Angle Regression

The LARS algorithm [**?**] is one of the methods that can be applied to compute sparse PCE models [**? ?**]. The key idea is to find the best set of polynomials from a given candidate set that minimizes the regularized form of (4.17):

$$\overline{\mathbf{w}} =_{\mathbf{w}} \mathbb{E}\left[\left(\mathbf{w}^T\mathbf{\Psi}(\mathbf{z}) - f(\mathbf{z})\right)^2\right] + \lambda||\mathbf{w}||_1. \tag{4.16}$$

The LARS algorithm in the context of PCE can be summarized as follows. We start with all PCE coefficients for the candidate polynomials set to zero, and find the polynomial, say $\Psi_1(\mathbf{w})$ most correlated with the model evaluations. This polynomial enters the active set. Next, we take the largest step in the direction of $\Psi_1(\mathbf{w})$ until some other polynomial $\Psi_2(\mathbf{w})$ from the candidate set, has as much correlation with the current residual. The second polynomial is now also added to the active set. In the next step, we move both the coefficients in the active set towards their least-square values until a third polynomial from the candidate set shows as much correlation as the current PCE model based on two polynomials shows with the model evaluations. The number of iterations is given by the minimum of $\{K, N\}$. After every iteration a posteriori error, for instance the Leave-One-Out (LOO) cross-validation error, is computed. The active set with the smallest LOO is then chosen as the best sparse PCE model.

One of the main advantage of the LARS algorithm is that it works well in cases when $K >> N$, i.e. the number of polynomials in the candidate set is much larger than the number of model evaluations.

4.3. Sobol index computation

5. Results

5.1. NM80

5.1.1. Operating conditions

As a reference wind turbine, we consider the 2MW NM80 turbine from the DANAERO project [23] with a blade radius of 38.8 m. Add operating conditions

5.1.2. Choice of uncertain inputs

The data for lift (C_l) and drag (C_d) polars are available at four locations along the blade radius at 11.87 m, 17.82 m, 28.97 m, and 35.53 m. The lift and drag variables at these sections are numbered Cl1 - Cl4 and Cd1 - Cd4 respectively. The reference value of these polars is obtained from the wind-tunnel experiment with 3D corrections. Random samples of chord, twist, lift- and drag-polars are obtained by perturbing the control points with a uniformly distributed random variable.

There are two ways to obtain perturbed curves: independently perturbing each of the control points (local perturbation) or using a single random number to perturb all the control points (global perturbation). We use local perturbation for chord control points Ch3 - Ch7 and twist control points Tw2 - Tw7 control points, see Fig. 3 (a) - (b), respectively. Each control point are perturbed using a uniform random number with bounds given by $\pm 5\%$ of the magnitude of a control point (see equation (**??**)). For the lift and drag curves, all control points are perturbed using the same uniform random number resulting in samples of the lift and drag curves as shown in Fig. 3 (c) - (d), respectively. For simplicity, we only consider uniform distributions for perturbing the control points, however, we can also use other probability distributions for this purpose. Also note that when using a uniform distribution with bounds given by the relative magnitude of control points, we tend to obtain small perturbations for control points with values close to zero.

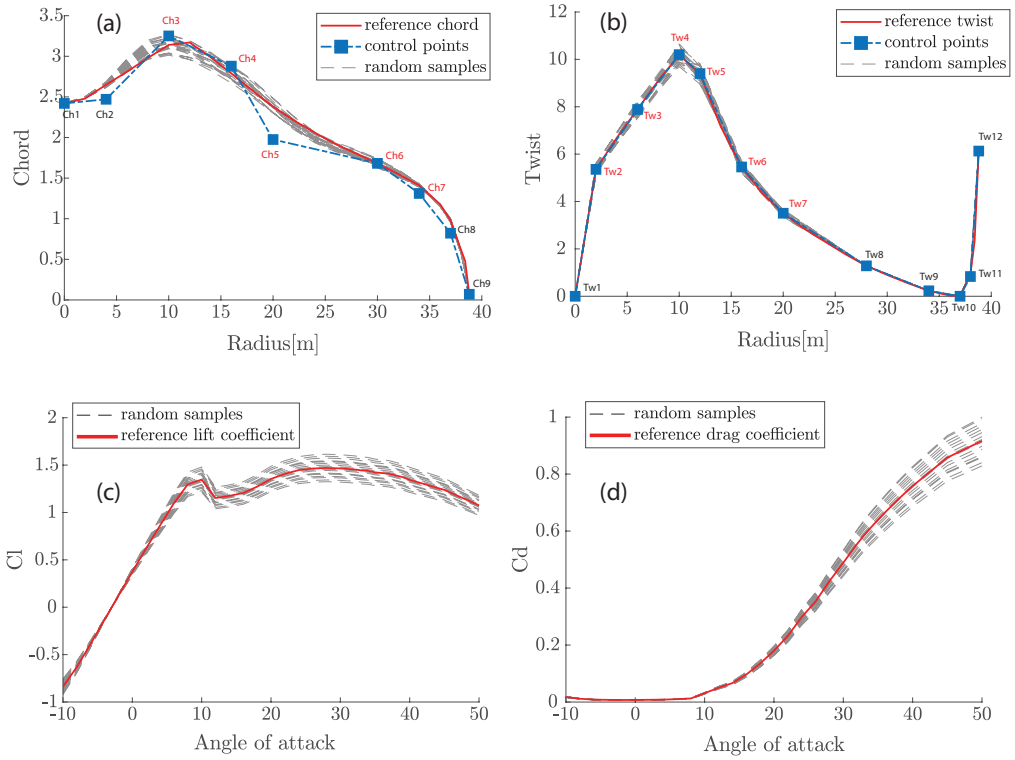

Figure 3: Random realization of chord, twist, lift- (Cl2) and drag-polars (Cd2).

5.1.3. *Verification of sensitivity analysis method*

We perform a convergence study for both OLS and LARS in order to determine which method converges fastest with increasing number of uncertain parameters and number of model runs. For this purpose we only include uncertainty in the chord. The NURBS representation is defined by 9 control points, of which a subset is taken uncertain (see Fig. 3(a)). In Fig. 4, we show for both OLS and LARS the convergence behaviour of the total Sobol indices of the power output with increasing number of model evaluations N (runs of the AeroModule), and with increasing number of uncertain inputs M (4, 6 and 8 control points). We see that both methods scale well with increasing dimensions, however, LARS exhibits faster convergence than OLS in high dimensions due to its adaptive nature, and will be the method of choice in the subsequent tests. what is a reasonable choice of N, depending on M?

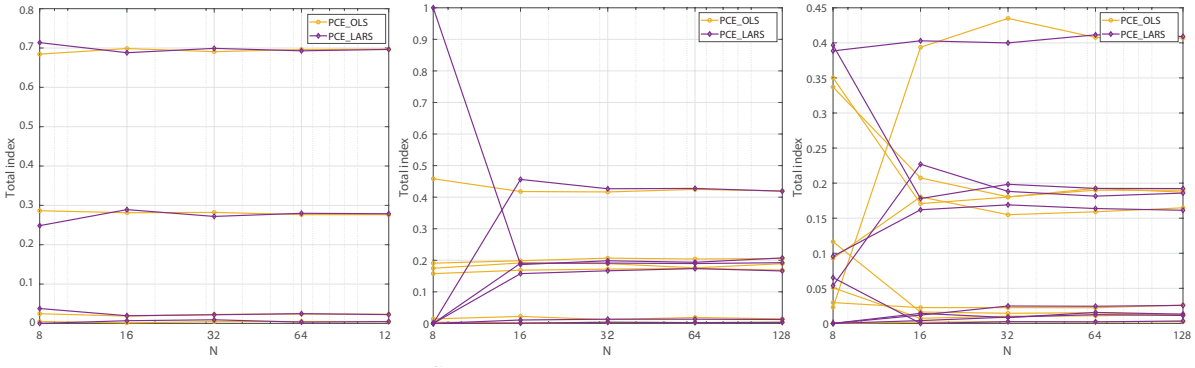

(a) $M = 4, Ch1 - Ch4$ **(b)** $M = 6, Ch1 - Ch6$ **(c)** $M = 8, Ch1 - Ch8$

Figure 4: Convergence of OLS and LARS with increasing number of uncertain inputs M and model evaluations N.

5.1.4. *Sensitivity analysis results*

In Fig. 5, we show the total order Sobol indices as a measure of the sensitivity of the different geometric and model parameters on the power output. In this case, we observe the important result that the uncertainty in model parameters is at least as important as the uncertainty in geometric parameters. Furthermore, within the geometric parameters, the chord distribution shows a significantly higher sensitivity compared to the twist variables

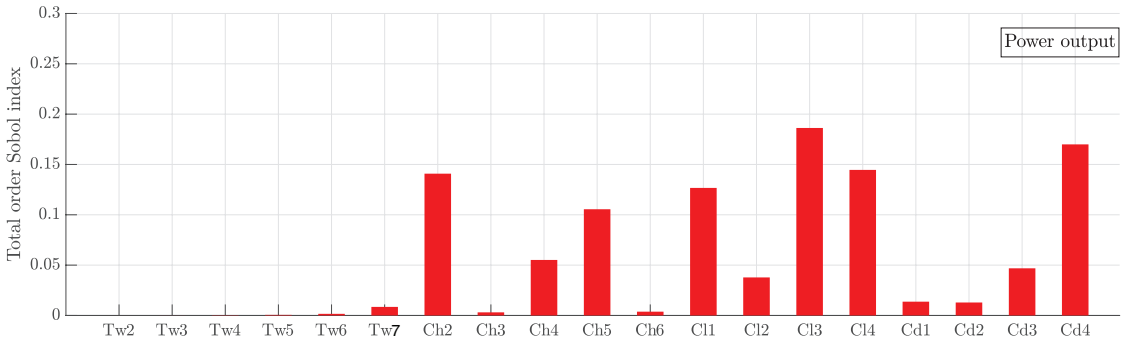

Figure 5

225 *5.2. AVATAR*

6. Conclusions

We have shown how Sobol indices computed using sparse adaptive polynomial expansion can be used for high-dimensional global sensitivity analysis of both geometric and model uncertainties. The identified sensitive model parameters will be utilized in future work to develop calibrated BEM models with built-in
230 uncertainty estimates as part of the *WindTrue* project, and is connected to IEA Task 29.

Acknowledgements

[1] K. Boorsma, F. Grasso, and J. Holierhoek. Enhanced approach for simulation of rotor aerodynamic loads. Technical Report ECN-M-12-003, 2012.

[2] P. Bortolotti, H. Canet, C. L. Bottasso, and J. Loganathan. Performance of non-intrusive uncertainty quantification in the aeroservoelastic simulation of wind turbines. *Wind Energy Science*, 4(3):397–406, 2019.

[3] C. L. Bottasso, A. Croce, L. Sartori, and F. Grasso. Free-form design of rotor blades. *Journal of Physics: Conference Series*, 524(1), 2014.

[4] T. Burton, N. Jenkins, D. Sharpe, and E. Bossanyin. *Wind Energy Handbook, Second Edition*. John Wiley & Sons, 2001.

[5] C. de Boor. *A Practical Guide to Splines*. In *Applied Mathematical Sciences*, 1978.

[6] K. Dykes, A. Ning, R. King, P. Graf, G. Scott, and P. Veers. Sensitivity Analysis of Wind Plant Performance to Key Turbine Design Parameters : A Systems Engineering Approach. *AIAA SciTech 2014*, (February), 2014.

[7] F. Echeverría, F. Mallor, and U. San Miguel. Global sensitivity analysis of the blade geometry variables on the wind turbine performance. *Wind Energy*, 20(9):1601–1616, sep 2017.

[8] A. J. Eggers, R. Digumarthi, and K. Chaney. Wind shear and turbulence effects on rotor fatigue and loads control. *Journal of Solar Energy Engineering, Transactions of the ASME*, 125(4):402–409, 2003.

[9] M. Fluck and C. Crawford. A fast stochastic solution method for the Blade Element Momentum equations for long-term load assessment. *Wind Energy*, 21(2):115–128, 2018.

[10] A. C. Hansen and C. P. Butterfield. Aerodynamics of horizontal-axis wind turbines. *Annual Review of Fluid Mechanics*, 25(1):115–149, 1993.

[11] A. Kusiak and Z. Zhang. Analysis of wind turbine vibrations based on SCADA data. *Journal of Solar Energy Engineering, Transactions of the ASME*, 132(3):0310081–03100812, 2010.

[12] H. A. Madsen, V. Riziotis, F. Zahle, M. Hansen, H. Snel, F. Grasso, T. Larsen, E. Politis, and F. Rasmussen. Blade element momentum modeling of inflow with shear in comparison with advanced model results. *Wind Energy*, 15(1):63–81, jan 2012.

[13] S. Marelli and B. Sudret. *UQLab: A Framework for Uncertainty Quantification in Matlab*, pages 2554–2563.

[14] D. Matthäus, P. Bortolotti, J. Loganathan, and C. L. Bottasso. Propagation of Uncertainties Through Wind Turbine Models for Robust Design Optimization. In *35th Wind Energy Symposium, AIAA SciTech Forum, 9-13 January 2017, Grapevine, Texas*, Reston, Virginia, jan 2017. American Institute of Aeronautics and Astronautics.

[15] P. M. McKay, R. Carriveau, D. S.-K. Ting, and J. L. Johrendt. *Global sensitivity analysis of wind turbine power output*. *Wind Energy*, 17(7):983–995, 2014.

[16] J. P. Murcia, P.-E. Réthoré, N. Dimitrov, A. Natarajan, J. D. Sørensen, P. Graf, and T. Kim. Uncertainty propagation through an aeroelastic wind turbine model using polynomial surrogates. *Renewable Energy*, 119:910–922, apr 2018.

[17] A. F. Ribeiro, A. M. Awruch, and H. M. Gomes. An airfoil optimization technique for wind turbines. *Applied Mathematical Modelling*, 36(10):4898–4907, 2012.

[18] J. M. Rinker. Calculating the sensitivity of wind turbine loads to wind inputs using response surfaces. *Journal of Physics: Conference Series*, 753(3), 2016.

[19] A. Robertson, L. Sethuraman, and J. M. Jonkman. *Assessment of Wind Parameter Sensitivity on Extreme and Fatigue Wind Turbine Loads*.

[20] D. F. Rogers. *An introduction to NURBS: with historical perspective*. Elsevier, 2000.

[21] M. Sayed, L. Klein, T. Lutz, and E. Krämer. The impact of the aerodynamic model fidelity on the aeroelastic response of a multi-megawatt wind turbine. *Renewable Energy*, 140:304–318, 2019.

[22] R. C. Smith. *Uncertainty Quantification: Theory, Implementation, and Applications*. Society for Industrial and Applied Mathematics, Philadelphia, PA, USA, 2013.

[23] N. Troldborg, C. Bak, H. A. Madsen, and W. Skrzypinski. Danaero mw: Final report. Technical Report DTU Wind Energy E-0027, 2013.

[24] L. M. M. van den Bos, W. A. A. M. Bierbooms, A. Alexandre, B. Sanderse, and G. J. W. van Bussel. Fatigue design load calculations of the offshore NREL 5MW benchmark turbine using quadrature rule techniques. pages 1–18, 2019.

[25] J. Velarde, C. Kramhøft, and J. D. Sørensen. Global sensitivity analysis of offshore wind turbine foundation fatigue loads. *Renewable Energy*, 140:177–189, 2019.

[26] F. Vorpahl, M. Strobel, J. M. Jonkman, T. J. Larsen, P. Passon, and J. Nichols. Verification of aero-elastic offshore wind turbine design codes under IEA Wind Task XXIII. *Wind Energy*, 17(4):519–547, apr 2013.

Appendix A. Literature overview of global sensitivity analysis in wind-turbine models

List of BEM codes in [21, 26].

Uncertainties and corrections in BEM models [12]: complex inflow, e.g. sheared inflow.

[8] study the effect of shear and turbulence on rotor loading, but not with a systematic (global) sensitivity analysis.

[15] perform a measurement data-only global sensitivity analysis using a neural network and a Fourier amplitude sensitivity test (a similar technique was used in [11] for vibration analysis). The neural network is constructed based on measurement data. The output quantity of interest is the power production; several input parameters are used, including yaw angle, rotor speed, blade pitch angle, wind speed, ambient temperature, main bearing temperature, wind speed standard deviation and yaw angle standard deviation.

[6] performed global sensitivity analysis of turbine costs with respect to key wind turbine configuration parameters including rotor diameter, rated power, hub height, and maximum tip speed. DAKOTA is used to calculate Sobol indices with Monte Carlo sampling.

[18] calculated the global sensitivity of wind turbine loads to wind inputs using polynomial response surfaces. She used Sobol indices, with quantity of interest the maximum blade root bending moment and as inputs four turbulence parameters: a reference mean wind speed, a reference turbulence intensity, the Kaimal length scale, and a parameter reflecting the nonstationarity. The turbine model studied is the WindPACT 5 MW reference model and the BEM model is FAST.

[7] employs a global sensitivity analysis to identify the design variables that affect wind turbine performance in order to reduce the number of variables in wind turbine design optimization. As input parameters, airfoil parameterization and chord and twist distributions are used; the outputs studied are annual energy production, maximum blade tip deflection, overall sound power level and blade mass. For example, Sobol indices are shown for the effect of chord and twist control points on the output quantities.

[14] performed uncertainty quantification including uncertainty in the aerodynamic properties; for example, the uncertainty in the lift coefficient at an airfoil section due to uncertain roughness (e.g. contamination) is achieved by interpolating between clean and fully rough state with a uniformly distributed random variable. Polynomial chaos and Kriging were used. See also [2], in which the AVATAR turbine was analysed, using the Cp-Lambda aeroelastic model and DAKOTA as UQ toolbox.

[16] similarly considered a global sensitivity analysis with Sobol indices computed by using sparse polynomial chaos expansion. The quantities of interest considered are the energy production and lifetime equivalent fatigue loads for the DTU 10 MW reference turbine. The uncertain input is given by the turbulent inflow field, with 4 parameters: mean hub height wind speed, std. dev. of hub height wind speed, shear exponent, yaw misalignment. The dependency between these parameters (as described by the Normal Turbulence Model) is taken into account by using a Rosenblatt transformation that transforms the dependent variables to a set of independent ones. The Chaospy package is used for the analysis. Seven different model outputs are considered: power, thrust, and several damage equivalent fatigue loads (EFL), computed using a rainflow counting algorithm. The sensitivity analysis shows that the turbulent inflow realization has a bigger impact on the total distribution of equivalent fatigue loads than the shear coefficient or yaw misalignment.

[21] argue that BEM models are accurate mainly for small turbines but that for large turbines, when the tip deformations exceed 10% of the blade radius, it is questionable if they can still be applied. They compare the results of engineering models to CFD-based aeroelastic simulations. It is shown that the 2D polars commonly used in BEM require 3D corrections, and that including more polars improves the results. ‘Turbine power and thrust predicted from the flexible rotor were reduced compared to the rigid rotor employing a BEM-based model. A reason behind the increase in power from the CFD-based model is the spanwise force component. It is not included in the BEM-based simulations as it is one of the main

assumptions of its theory. This assumption could be used for small wind turbine simulations where the edgewise deformations were insignificant. But for such large wind turbines, the spanwise force distribution over the blade radius must be taken into account in the calculation of the power output due to the large edgewise deformations. To increase the accuracy of the engineering model, it is recommended to increase the number of polars calculated by 2D CFD simulations at different sections along the blade. This is because of the significant difference in the Reynolds number for the large blade.'

[25] perform a global sensitivity analysis of fatigue loads with respect to structural, geotechnical and metocean parameters for a 5MW offshore wind turbine installed on a gravity based foundation. Linear regression of Monte Carlo simulations and Morris screening are performed for three design load cases.

[19] assesses the sensitivity of different wind parameters on the loads of a wind turbine. They argue that the most common parameters considered normally in literature are the turbulence intensity variability, and the shear exponent, or wind profile, both having important influence on the turbine response. In the paper an assessment of which wind characteristics influence wind turbine structural loads is given. The correlated dependency between the individual parameters is not considered; rather, they focus on assessing the sensitivity of each parameter individually. An elementary-effects screening method (Morris screening) is used as global sensitivity method. The NREL 5MW turbine and FAST are used.

[9] develop an *intrusive* stochastic BEM method: 'a stochastic solution for the unsteady aerodynamic loads based on a projection of the unsteady Blade Element Momentum (BEM) equations onto a stochastic space spanned by chaos exponentials'.

[**?**] used global sensitivity analysis (as part of a four-step approach) to reduce the parameter dimension for structural behaviour computations using FAST as aeroelastic code. The methods of expert knowledge, one-at-a-time variation, and regression based on Monte Carlo sampling are used as pre-processing steps to reduce the computational expense of global sensitivity analysis.